TISSUE ENGINEERING: Part A
Volume 23, Numbers 11 and 12, 2017

DOI: 10.1089/ten.tea.2016.0494

termis
Tissue Engineering
& Regenerative Medicine
International Society

ORIGINAL ARTICLE

NANOG Restores Contractility of Mesenchymal Stem Cell-Based Senescent Microtissues

Aref Shahini, BS,[1,*] Panagiotis Mistriotis, PhD,[1,*] Mohammadnabi Asmani, MS,[2] Ruogang Zhao, PhD,[2] and Stelios T. Andreadis, PhD[1–3]

Mesenchymal stem cells (MSCs) have been extensively used in the field of tissue engineering as a source of smooth muscle cells (SMCs). However, recent studies showed deficits in the contractile function of SMCs derived from senescent MSCs and there are no available strategies to restore the contractile function that is impaired due to cellular or organismal senescence. In this study, we developed a tetracycline-regulatable system and employed micropost tissue arrays to evaluate the effects of the embryonic transcription factor, NANOG, on the contractility of senescent MSCs. Using this system, we show that expression of NANOG fortified the actin cytoskeleton and restored contractile function that was impaired in senescent MSCs. NANOG increased the expression of smooth muscle α-actin (ACTA2) as well as the contractile force generated by cells in three-dimensional microtissues. Interestingly, NANOG worked together with transforming growth factor-beta1 to further enhance the contractility of senescent microtissues. The effect of NANOG on contractile function was sustained for about 10 days after termination of its expression. Our results show that NANOG could reverse the effects of stem cell senescence and restore the myogenic differentiation potential of senescent MSCs. These findings may enable development of novel strategies to restore the function of senescent cardiovascular and other SMC-containing tissues.

Keywords: senescence, aging, stem cells, NANOG, ACTIN cytoskeleton, smooth muscle contraction

Introduction

Mesenchymal Stem Cells (MSCs) have been widely investigated in clinical trials to treat multiple degenerative diseases, including neurological disorders, inflammation, brain and spinal cord injury, kidney, skin, or cardiac diseases.[1–3] While clinical trials require large quantities of high-quality MSCs (sometimes up to 10^{10} cells per treatment[4]), several studies showed that proliferation and differentiation potential of MSCs depend heavily on donor age.[5–9] In addition, culture senescence limits MSC culture time to less than 8–10 passages, preventing their expandability to the large cell numbers required for cellular therapies.[10,11] This is a major concern as the patients mostly in need for cellular therapies are elderly.

Smooth muscle cells (SMCs) are critical building blocks of several organs such as blood vessels, bladder, intestine, skin, and eyes. Their primary function is to contract and relax to regulate diverse tissue and organ functions, including digestion, urination and blood flow, erection of skin hair, and keeping the upper eyelid open among others. However, SMC function is highly compromised during aging. Aortic SMCs isolated from old mice generated less force than young SMCs as demonstrated by collagen contraction assay.[12] SMCs in aged arteries also become senescent or die due to apoptosis.[13,14] Other studies have reported that aged SMCs secrete matrix metalloproteinases that degrade extracellular matrix[15,16] and proinflammatory cytokines[17] that attract immune cells and induce proliferation[18,19] and oxidative stress.[20]

MSCs can be successfully applied toward the development of functional contractile tissues due to their high proliferation and multilineage differentiation potential. In fact, it has been shown that human adult MSCs can effectively differentiate into SMCs that were applied to engineer functional arterial substitutes as well as other SMC-containing tissues.[21–24] However, cellular and organismal aging severely reduces the myogenic capacity of MSCs.[8] Therefore, developing a strategy to enhance the contractile properties of senescent stem

[1]Bioengineering Laboratory, Department of Chemical and Biological Engineering, University at Buffalo, The State University of New York, Amherst, New York.
[2]Department of Biomedical Engineering, University at Buffalo, The State University of New York, Amherst, New York.
[3]Center of Excellence in Bioinformatics and Life Sciences, Buffalo, New York.
*Equal contribution.

cells is highly desired. Interestingly, recent work in our laboratory showed that ectopic expression of a single pluripotent transcription factor, NANOG, could reverse aging and restore the impaired contractility of aged adult MSCs.[25,26]

In this study, we sought to identify the effects of NANOG on the force generation capacity of MSCs in a three-dimensional (3D) microenvironment. To this end, we generated a tetracycline-regulatable vector that tightly controls the expression of NANOG by the addition or withdrawal of the tetracycline analog, doxycycline (DOX). To measure the contractile force, we applied microfabricated tissue gauges containing micropillars that can act as a force sensor while, at the same time, enabling visualization of cells within the 3D constructs.[27] Using this system, we discovered that the expression of NANOG restored the impaired contractility of senescent microtissues by restoring the ability of cells to form the actin cytoskeleton.

Materials and Methods

Cultivation of HF-MSCs, cloning, and lentivirus transduction

Human hair follicle MSCs were isolated from a 73-year-old donor[28] and cultured up to passage 14. Based on our previous study, the cells were defined as early passage (EP) before passage 8 and late passage (LP) after passage 14, representing young and senescent cells, respectively.[28] Human dermal fibroblasts were derived from neonatal foreskin as described previously.[29] Human aortic vascular SMCs (VSMCs) were purchased from ATCC (Manassas, VA). Cells were cultured in growth medium comprising Dulbecco's modified Eagle's medium (Gibco, Grand Island, NY) supplemented with 10% FBS (Gibco). Cells were passaged every 4 days using 0.25% trypsin (Gibco). SMC and human fibroblast contraction experiments were performed at passage 9.

The plasmid for reverse tetracycline transactivator (rtTA) was purchased from Addgene (Cambridge, MA). Cloning of NANOG or ZsGreen into the tetracycline controlled (Tet-On) lentiviral vector pNL-EGFP/TREPittdU3 (Addgene), resulting in pTRE-NANOG-IRES-PURO or pTRE-ZsGreen-IRES-PURO as described previously.[30] Recombinant lentiviruses encoding for rtTA, NANOG, or ZsGreen were produced using these plasmids as described elsewhere.[31] Cells were co-transduced with NANOG- or ZsGreen-encoding virus and the virus encoding for rtTA. NANOG or ZsGreen expression was induced by DOX (BD, Franklin Lakes, NJ) at a final concentration of 1 μg/mL in the culture medium, unless stated otherwise. Cells that were cultured in the absence of DOX were considered as control (Ctr). Before seeding the microdevice, cells were cultured in the presence of DOX for 5 days unless stated otherwise.

Microdevices to measure contractile properties

To measure contractility, we manufactured a microdevice that contains an array of 13×10 microwells, each containing two micropillars with heads, using multilayer microlithography, as described previously.[27] Briefly, SU-8 photoresist was used to create the first layer on silicon wafer. This layer constitutes the base of the micropillar. After exposing the base layer to UV light, the head section (top layer) of the micropillar was spun on top and exposed to UV through the mask. Both head and bottom patterns were exposed to 365 nm UV light at 10 mJ/cm^2 intensity for 20 and 50 s, respectively. A blocking photoresist layer in between the top and base layers was cast off to prevent unwanted cross-linking of the first layer. Next, the micropillar array pattern was transferred to polydimethylsiloxane (PDMS, Sylgard 184; Dow-Corning, Midland, MI) through replica molding. The final device was casted in a P35 Petri dish using PDMS stamps.

To seed microtissues in the micropillar array, arrays were sterilized in 70% ethanol and then treated with 0.2% Pluronic F127 (BASF, Florham Park, NJ) to form a hydrophobic barrier between the PDMS surface and collagen and prevent collagen from attaching to the PDMS surface. Next, rat tail collagen type I (Corning®, Riverfront Plaza, NY) was neutralized by NaOH (1 M), mixed with cells (3×10^5 cells per device), and immediately seeded on the device. Microtissues were formed in between the two micropillars and contractile forces were measured after 24 h unless otherwise stated. To this end, images were taken from top and bottom (stationary part) of the micropillars using $10\times$ objective on an Olympus IX81 microscope (Center Valley, PA). Next, the deflection of micropillar heads from the stationary base was measured using ImageJ software and multiplied by the pillar's spring constant (2.2 ± 0.1 μN/μm) to calculate the force.[27] Contractile force was normalized to the total cell number in each microtissue.

Western blot analysis

Cells grown on tissue culture plates were lysed using lysis buffer: 62.5 mM Tris-HCl (pH 6.8 at 25°C), 2% (w/v) sodium dodecyl sulfate (SDS), 10% (v/v) glycerol, 0.1% (w/v) bromophenol blue, supplemented with 41.67 mM dithiothreitol (Cell Signaling, Danver, MA), and protease inhibitor cocktail (Sigma-Aldrich, St. Louis, MO). Protein lysates were denatured at 95°C for 5 min and separated based on their molecular weight by 8% or 10% SDS-polyacrylamide gel electrophoresis. Proteins were transferred to nitrocellulose membranes (Trans-Blot Turbo Transfer System; Bio-Rad, Hercules, CA) and probed for specific proteins using antibodies against NANOG (1:1000 in 5% (w/v) bovine serum albumin; BD) and ACTA2 (1:2000 dilution in 5% (w/v) nonfat dry milk; Sigma-Aldrich). The antibody against glyceraldehyde-3-phosphate dehydrogenase (GAPDH, 1:10,000 dilution in 5% (w/v) nonfat dry milk; Cell Signaling) was used to determine the total amount of protein loaded. Protein bands were detected using horseradish peroxidase-labeled secondary antibodies and a chemiluminescence kit (LumiGLO; Cell Signaling) as per manufacturer's instructions. The protein levels of NANOG and ACTA2 were quantified by measuring the band intensities using ImageJ software and normalized to the intensity of GAPDH. The lysate concentration and exposure time were chosen to ensure that the signal was in the linear range.

Immunocytochemistry

To observe the organization of actin filaments, immunostaining for F-actin using phalloidin stain and ACTA2 using ACTA2 antibody was performed on the 3D microtissues or cells cultured in two dimensions. Briefly, cells or microtissues were fixed in 4% (w/v) paraformaldehyde for 10 min at 25°C, permeabilized by incubating with 0.1% (v/v) Triton X-100/PBS for 10 min at 25°C, and blocked with 5% (v/v) goat serum in 0.01% (w/v) Triton X-100/PBS at 25°C for 1 h. To

probe for ACTA2 and MRTF-A, the cells were incubated overnight at 4°C with the following antibodies diluted in blocking buffer: mouse anti-human α-smooth muscle (1:100, A5228; Sigma-Aldrich) and rabbit anti-human MRTF-A (1:200; Santa Cruz, Dallas, TX). Subsequently, the cells were incubated for 1 h at 25°C with Alexa Fluor 488-conjugated goat anti-mouse or goat anti-rabbit antibodies diluted in blocking buffer (1:100; Thermo Fisher Scientific, Waltham, MA) and counterstained with Hoechst 33342 nuclear dye for 5 min (1:400 dilution in PBS; Thermo Fisher Scientific). F-actin staining was performed using Alexa Flour 594 phalloidin (1:50 dilution in PBS +1% (w/v) bovine serum albumin; Thermo Fisher Scientific) as per manufacturer's instructions. Fluorescent images were acquired using the Zeiss Axio Observer Z1 (LSM 510; Zeiss, Oberkochen, Germany) equipped with a digital camera (ORCA-ER C4742-80; Hamamatsu, Bridgewater, NJ). Immunostaining for MRTF-A nuclear translocation was quantified using ImageJ software by measuring the intensity of the MRTF-A signal colocalized with the Hoechst nuclear stain.

RNA isolation, cDNA synthesis, and quantitative real-time polymerase chain reaction

To analyze the mRNA expression profile of *ACTA2* after expression and removal of NANOG, the total RNA was isolated from cells plated on tissue culture plates using the RNeasy Mini Kit (QIAGEN, Valencia, CA) as per manufacturer's instructions. Subsequently, cDNA was synthesized from total RNA using the QuantiTect Reverse Transcription Kit (QIAGEN). Quantitative real-time polymerase chain reaction (RT-PCR) was performed using the SYBR Green Kit (Bio-Rad) according to the manufacturer's instructions and specific primers for each gene as follows:

ACTA2 (forward: 5′-GACAGCTACGTGGGTGACGAA-3′; reverse: 5′-GATGCCATGTTCTATCGGGTACT-3′);

MYL9 (forward: 5′-TGACAAGGAGGACCTGCAC-3′; reverse: 5′-CATCATGCCCTCCAGGTATT-3′);

ACTG2 (forward: 5′-CGTGACCTCACGGACTACCT-3′; reverse: 5′-TGTGGCCATCTCATTCTCAA-3′);

TAGLN (forward: 5′-ATGGCCAACAAGGGTCC-3′; reverse: 5′-CTTCAAAGAGGTCAACAG-3′);

MYH11 (forward: 5′- CGCCAAGAGACTCGTCTGG-3′; reverse: 5′-TCTTTCCCAACCGTGACCTTC-3′); and

RPL32 (forward: 5′-AGCGTAACTGGCGGAAAC-3′; reverse: 5′-CGTTGTGGACCAGGAACTTC-3′).

The mRNA expression level was quantified using the ΔC_T method and normalized to the expression level of the housekeeping gene, *RPL32*.

Statistical analysis

Data are shown as mean ± standard deviation (SD). For the kinetics of gene expression, we performed analysis of variance (one-way ANOVA), followed by Fisher's least significant difference as a *post hoc* analysis. The statistical significance between two mean values was analyzed using two-tailed unpaired Student's *t*-test with respect to the standard deviations. Probability values less than 0.05 ($p < 0.05$) were considered statistically significant. Forces were measured from at least 20 microtissues per condition in each experiment and all experiments were repeated three independent times.

Results

NANOG enhances the contractile force generated by 3D tissue constructs

First, we evaluated the force generation capacity of several contractile cell types such as human hair follicles derived MSCs at EP, VSMCs, and fibroblasts. To this end, cells were embedded in collagen gels (3×10^5 cells per device) and allowed to polymerize in microwells, each containing a pair of flexible microposts (Fig. 1A, B), and the force exerted by the cells in each microtissue was calculated by micropost displacement using Hooke's law (Fig. 1C). Our results show that the contractile force of VSMC-based microtissues (1489 ± 278 nN/cell) was significantly higher than the force generated by EP MSCs (200 ± 53 nN/cell), while 5 days of transforming growth factor-beta (TGF-β1) treatment enhanced the contractile force of MSCs to 561 ± 113 nN/cell. The force generated by fibroblasts (422 ± 79 nN/cell) was also higher than MSCs, but still significantly lower than VSMCs and MSC+TGF-β1 (Fig. 1D).

Previous work from our laboratory showed that ectopic expression of the pluripotent transcription factor NANOG increased the myogenic differentiation and contractile capacity of SMCs derived from senescent MSCs.[25,30] Therefore, we examined whether NANOG could increase the force generation capacity of 3D senescent tissue constructs.[27] To this end, we developed a tetracycline-regulatable lentiviral system that enabled expression of NANOG upon addition of DOX to the culture medium. Hair follicle (HF)-derived MSCs were transduced at an EP and NANOG was expressed in senescent cells (LP cells) upon addition of DOX in the medium. Senescent cells that were cultured in the absence of DOX were used as Ctr throughout the study.

We found that senescent microtissues, that is, microtissues containing LP cells, expressed significantly lower amount of ACTA2 (Fig. 1E, F) and produced significantly lower contractile force (LP = 77 ± 62 nN/cell) compared with microtissues prepared with EP cells (EP = 179 ± 36 nN/cell) (Fig. 1G). Interestingly, expression of NANOG restored ACTA2 expression and actin filament formation, as well as the contractile function of senescent cells (LP-NANOG = 289 ± 74 nN/cell) (Fig. 1E–G). Cell-mediated contraction of collagen gels occurred rapidly and reached a plateau as soon as 6 h after seeding, but the results were more consistent at 24 h (Supplementary Fig. S1A; Supplementary Data are available online at www.liebertpub.com/tea). Therefore, we chose to perform force measurements at 24 h after cell seeding for the rest of our experiments. We also employed MSCs that were engineered to express ZsGreen (ZsG, a brighter version of GFP) in a DOX-regulatable manner. Upon treatment with DOX, ZsG-expressing microtissues generated similar force as Ctr microtissues (transduced with the NANOG gene, but not treated with DOX) (Supplementary Fig. S1B), suggesting that improved contraction was not affected by DOX, but was solely due to NANOG expression.

NANOG expression and microtissue contraction increased with increasing DOX concentration

Next, we determined the effect of NANOG concentration on force generation. To this end, cells were treated with the indicated concentrations of DOX for 5 days before

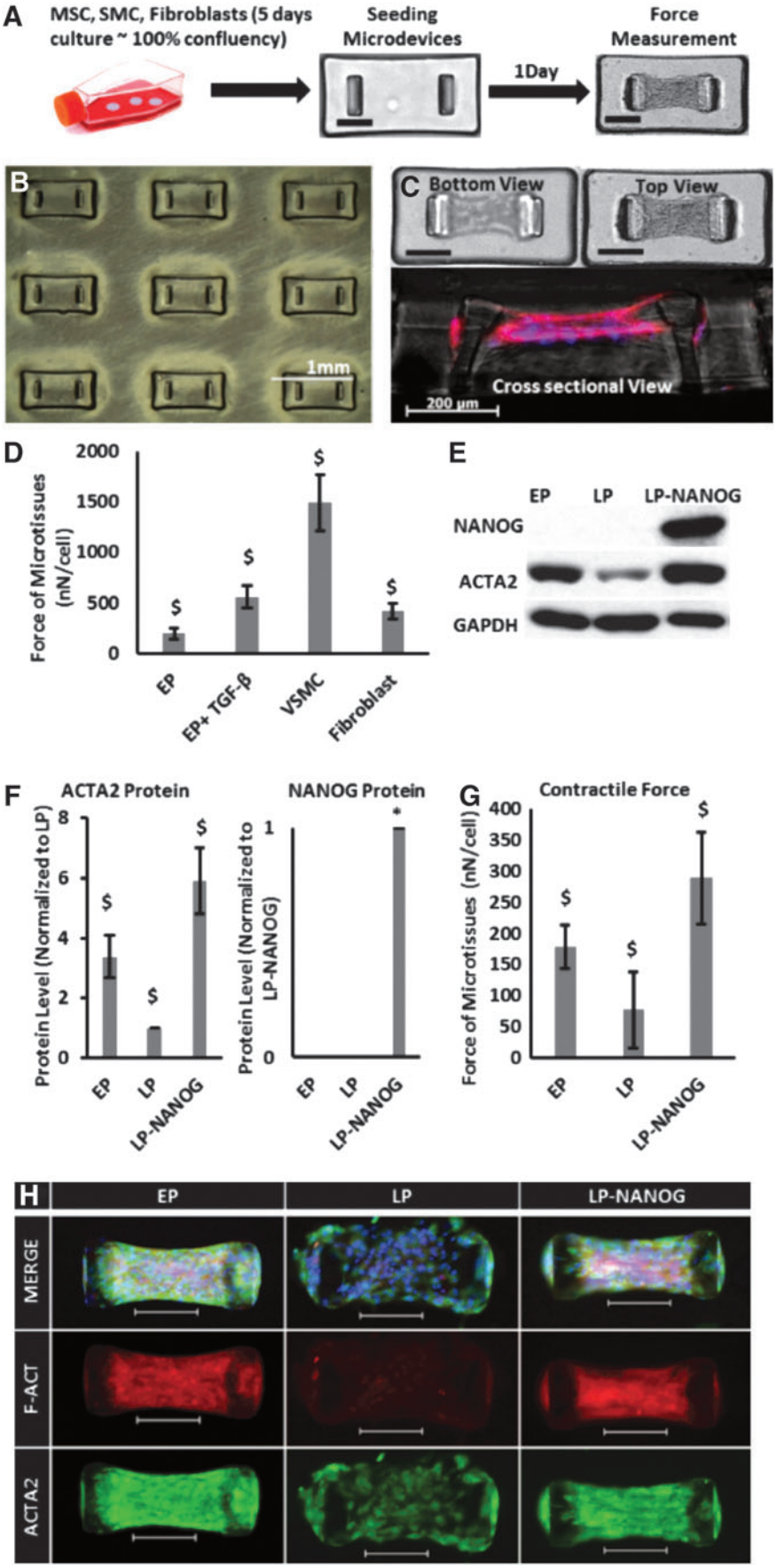

FIG. 1. Restoring the contractile function of senescent cells by NANOG expression. **(A)** Schematic representation of the experimental setup (scale bar = 200 µm). **(B)** Low-magnification picture from the array of microwells. **(C)** Bottom, top, and cross-sectional views of a microtissue (scale bar = 200 µm). **(D)** Forces generated by human EP MSCs, VSMCs, and fibroblasts. **(E, F)** Western blotting and quantification of ACTA2 and NANOG proteins for EP, LP, and LP-NANOG MSCs. **(G)** Contractile force generated by EP, LP, and LP-NANOG. **(H)** Immunofluorescence images of EP, LP, and LP-NANOG tissues stained for ACTA2 and F-actin (scale bar = 200 µm). Data are presented as mean ± standard deviation, $n = 3$ for WB quantification and $n = 20$ for force measurements. $ denotes $p < 0.05$ compared with all other samples, * denotes $p < 0.05$ compared with control. EP, early passage; LP, late passage; MSC, mesenchymal stem cell; VSMC, vascular smooth muscle cell.

embedding them into the collagen hydrogels to form microtissues. We found that increasing the concentration of DOX resulted in increased expression of NANOG and led to increased expression of the prototypical myogenic marker ACTA2 (Fig. 2A, B). At 1 μg/mL of DOX, NANOG expression reached a plateau and ACTA2 expression increased ninefold compared with Ctr (0 μg/mL DOX). In addition to increased expression, confocal immunofluorescence microscopy showed that NANOG expression induced ACTA2 and F-actin polymerization and filamentous organization, indicative of contractile SMC phenotype (Fig. 2C). Finally, the magnitude of the contractile force increased in a DOX concentration-dependent manner from 72 ± 41 nN/cell at 0 μg/mL to 321 ± 63 nN/cell at 1 μg/mL of DOX (Fig. 2D).

Effect of temporal expression of NANOG on the contractile force of microtissues

Next, we examined whether the time period of NANOG expression affected the level of force generated by microtissues. To this end, MSCs were cultured in the presence of DOX (1 μg/mL) for different times as indicated (between 1 and 5 days) and then embedded in collagen gels at the same time to form microtissues. As shown in Figure 3A, all cells were cultured for 5 days and all microtissues were cultured for 24 h. Interestingly, NANOG protein level reached saturation after 1-day treatment with DOX, while the ACTA2 protein level gradually increased by 3-, 7-, and 11-fold after 2, 4, and 5 days, respectively (Fig. 3B, C). Similarly, filamentous organization of actin also increased with time of DOX treatment, reaching maximum on day 4 (Fig. 3D). Accordingly, the force generated by the tissues also increased with time of DOX treatment, from 72 ± 36 nN/cell (no DOX) to 156 ± 42 nN/cell after 1 day to 237 ± 63 nN/cell after 3 days of DOX treatment and remained at that level thereafter (Fig. 3E).

Additive effects of NANOG and TGF-β1 on contractile function of senescent microtissues

Previous studies have shown that TGF-β1 induced formation of actin filaments and contractility in MSCs.[32–34] Therefore, we examined whether NANOG and TGF-β1 might increase contractility in an additive manner. To this end, we cultured MSCs in the presence of 1 μg/mL DOX and 2 ng/mL TGF-β1 for 5 days before measuring contractile force exerted by the microtissues.

While NANOG or TGF-β1 increased the contractile force significantly, the effect of NANOG was more pronounced than that of TGF-β1 (NANOG: 279 ± 52; TGF-β1: 195 ± 62; Ctr: 92 ± 51 nN/cell). Interestingly, the combination of NANOG and TGF-β1 increased the level of force even further to 529 ± 78 nN/cell (Fig. 4A). In agreement, the combination of TGF-β1 and NANOG also increased the expression level and filamentous organization of actin over either NANOG or TGF-β1 alone (Fig. 4B–D).

The effects of NANOG persist for several days after DOX removal

Next, we examined whether the effects of NANOG are transient or whether they persist when NANOG expression is terminated. To this end, cells were treated with DOX

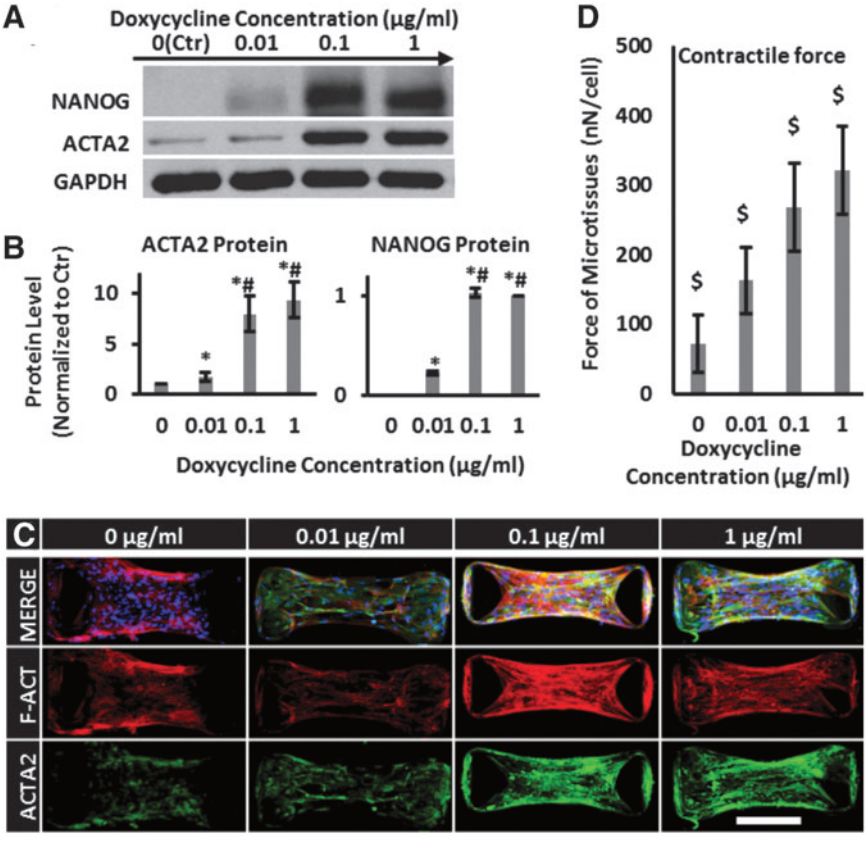

FIG. 2. NANOG increased the contractile force of senescent microtissues. MSCs were treated with the indicated DOX concentrations and the contractile force was measured using micropost devices. **(A, B)** Western blotting analysis and quantification of NANOG and ACTA2 protein levels as a function of DOX concentration. **(C)** Confocal immunofluorescence microscopy of microtissues stained for ACTA2 (*green*) protein and F-actin (*red*) at the indicated DOX concentrations (scale bar = 200 μm). **(D)** Contractile force as a function of DOX concentration. Data are presented as mean ± standard deviation, $n = 3$ for WB quantification and $n = 20$ for force measurements. $ denotes $p < 0.05$ from all other samples, * denotes $p < 0.05$ compared with 0 μg/m, and # denotes $p < 0.05$ compared with 0.01 μg/mL DOX. DOX, doxycycline.

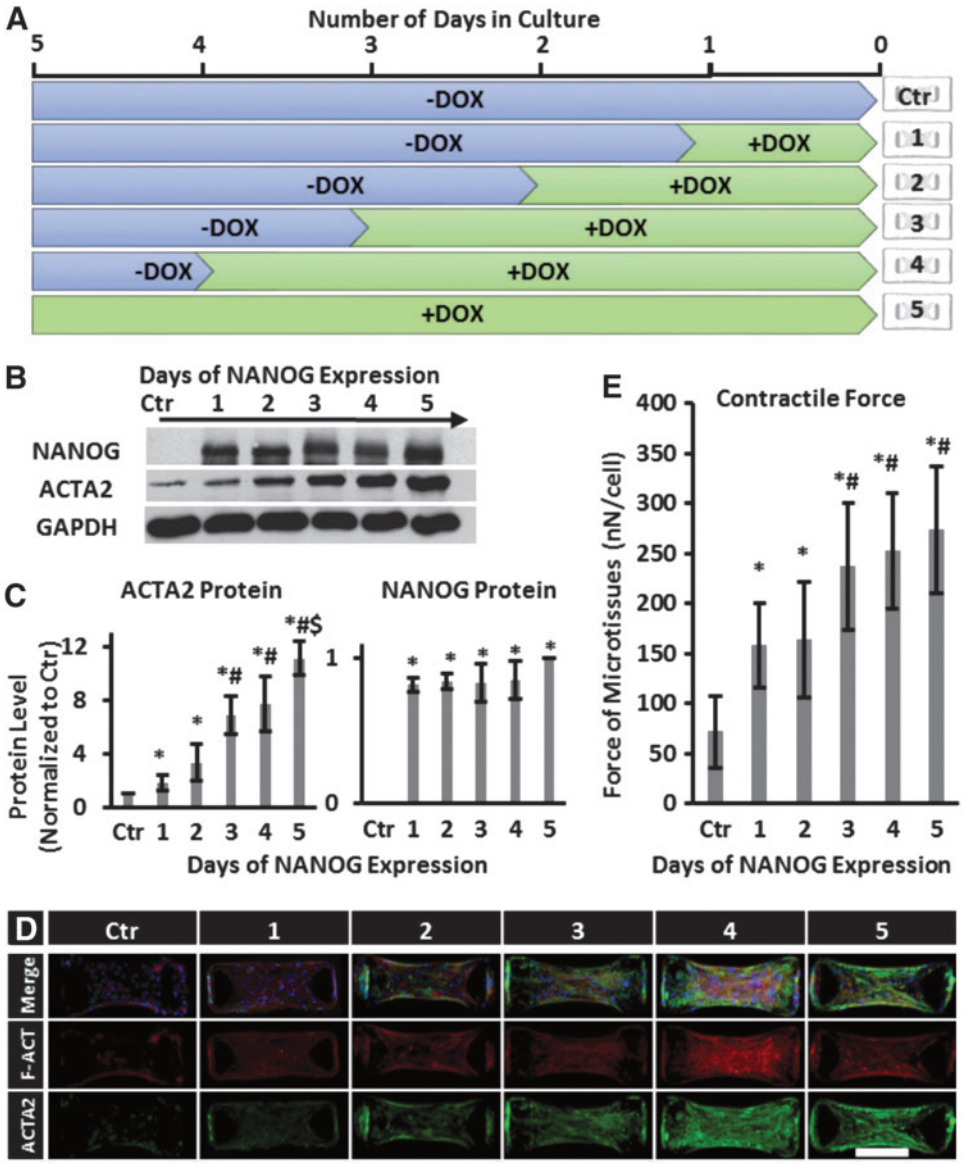

FIG. 3. Effect of time of NANOG expression on the contractile force of MSCs. **(A)** Schematic illustration of the experimental design. MSCs were cultured in the presence of 1 μg/mL DOX for 1 to 5 days and subsequently seeded in the microdevices for 24 h. **(B, C)** Western blot and quantification of NANOG and ACTA2 protein levels. **(D)** Immunostaining of microtissues for F-actin (*red*) and ACTA2 (*green*) (scale bar = 200 μm). **(E)** Contractile force as a function of the time of DOX treatment. * denotes $p < 0.05$ compared with control; # denotes $p < 0.05$ compared with 1 and 2 days; and $ denotes $p < 0.05$ compared with 4 days of NANOG expression. Data are presented as mean ± standard deviation, $n = 3$ for WB quantifications and $n = 20$ for force measurement.

(1 μg/mL) to induce NANOG expression for a 5-day window and then DOX was removed for the subsequent 0, 5, 10, or 20 days (Fig. 5A). All microtissues were prepared on day 20 and cultured for 24 h before they were tested. Interestingly, the level of NANOG decreased rapidly upon removal of DOX (half-life $\sim 2.5 \pm 0.5$ h) and was barely detectable by 10 h (Fig. 5B). Despite the short half-life of NANOG, the ACTA2 protein level was sustained up to 5 days and decreased significantly (40% decrease, $n = 3$, $p < 0.05$) by day 10 and even further by day 20 (60% decrease, $n = 3$, $p < 0.05$) compared with the level on day 0 (Fig. 5C). The contractile force was sustained up to 10 days following DOX withdrawal and decreased to levels of Ctr tissues after 20 days (Fig. 5D).

It is known that upon actin polymerization, MRTF-A is released from G-actin and translocates to nucleus, where the MRTF-A/SRF complex affects expression of cytoskeletal genes.[35] To begin to understand how the force generation capacity of microtissues could persist in the absence of NANOG, we examined actin polymerization by following the nuclear localization of MRTF-A. Briefly, the cells were treated with DOX for 5 days, then serum starved for 24 h, and stimulated with media containing 10% serum for 10 min. As shown in Figure 6A, B, MRTF-A nuclear translocation and actin polymerization remained significantly higher than the control up to 5 days after removal of DOX, suggesting that actin polymerization continued during that time. On the other hand, quantitative real-time RT-PCR also showed that the mRNA levels of *ACTA2*, *ACTG2*, *TAGLN*, *MYH11*, and *MYL9* increased significantly upon NANOG expression, but decreased rapidly and reached control levels by 48 h after DOX removal (Fig. 6C–G). These data show that the transcription of myogenic genes decreased quickly upon termination of NANOG expression, but actin polymerization and therefore contractile function were sustained for several days.

Discussion

MSCs are a promising source for vascular tissue engineering and regeneration due to their proliferation and

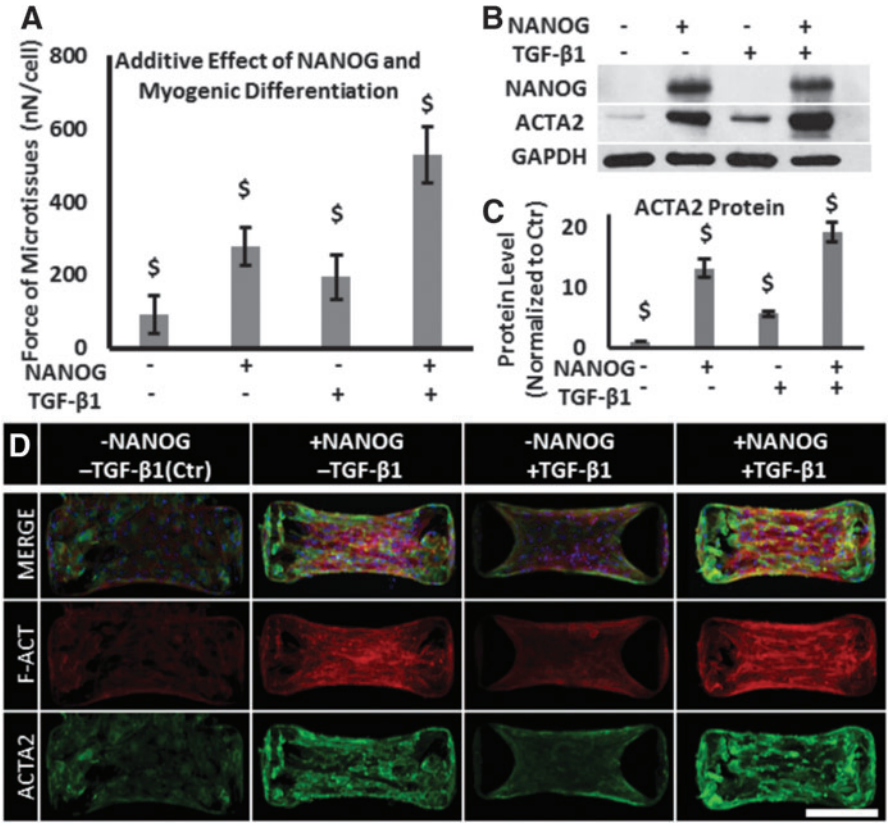

FIG. 4. Additive effects of NANOG and TGF-β1 on restoring the contractile function of senescent microtissues. **(A)** Effects of NANOG, TGF-β1, or both on the contractile force of microtissues. **(B, C)** Protein level of ACTA2 in the presence of NANOG, TGF-β1, or both as measured by western blot. **(D)** Confocal immunofluorescence microscopy of microtissues for ACTA2 (*green*) protein and F-actin (*red*) (scale bar = 200 μm). Data are presented as mean ± standard deviation, $n = 3$ for WB and $n = 20$ for force measurement. $ denotes $p < 0.05$ compared with all other samples. TGF-β1, transforming growth factor-beta1.

smooth muscle differentiation capacity.[21–24,34,36–38] However, organismal aging or culture senescence impairs the myogenic differentiation of MSCs.[8] We demonstrated that aged myogenic progenitors lose their capacity to activate key myogenic pathways, resulting in impaired contractile function.[30] The loss of stem cell function is a major concern since the majority of patients in need for cellular therapies are elderly.

Current strategies to enhance the myogenic differentiation and contractile function include extracellular signaling factors,[8,34,39, 40] cell–cell[41] and cell–matrix[42] interactions, and application of pulsatile forces.[43,44] However, TGF-β1 treatment can only partially restore the contractile function of senescent cells[8,30] and the effect of mechanical pulsation on contractile properties is also cell type dependent and hair follicle MSCs do not respond to this stimulation.[44] As for the other strategies, it remains to be determined whether they can be employed to reverse the loss of contractile function due to aging. Interestingly, we reported previously that ectopic expression of the pluripotent transcription factor NANOG was sufficient to reverse cellular senescence and restore the impaired myogenic differentiation of senescent MSCs.[25] In the current study, we investigated the effect of NANOG on the contractile function of senescent MSCs in 3D microtissues, which enabled direct measurement of contractile forces using a microtechnology platform. Our results show that expression of NANOG restored the actin cytoskeleton that was absent in senescent microtissues and increased the contractile force in NANOG concentration-dependent manner. Interestingly, NANOG works together with TGF-β1 to further enhance actin polymerization and the contractile properties of senescent cells. Finally, despite the short half-life of NANOG protein, the effect of NANOG on the contractile function was sustained up to 10 days after the expression of NANOG terminated, indicating that structural changes in the cells persisted for days in the absence of NANOG.

Generating contractile force requires actin polymerization and filamentous organization, which are essential to formation of actomyosin machinery and contraction.[45,46] Indeed, expression of NANOG rapidly restored both F-actin and ACTA2 filament formation, which was significantly compromised in senescent cells. As a result, the force of contraction also increased after only 1 day of NANOG expression and reached maximum levels after ~3 days. The contractile function correlated with the amount and organization of actin filaments, which were significantly enhanced upon expression of NANOG. Our recent results suggested that NANOG exerted its effects by activating the ROCK pathway, resulting in actin polymerization, MRTF-A translocation into the nucleus, and subsequent SRF-dependent myogenic gene expression.[30] Therefore, the effects on actin cytoskeleton may be a part of a broader response of senescent cells to NANOG.

Interestingly, the effects of NANOG were further enhanced by treatment with TGF-β1, which is known to increase ACTA2 expression and myogenic differentiation.[8,38] Upon expression of NANOG or addition of TGF-β1, the contractile force increased by approximately fourfold and twofold, respectively. However, the combination of NANOG and TGF-β1 increased the force by approximately eightfold, suggesting that the two factors act in an additive

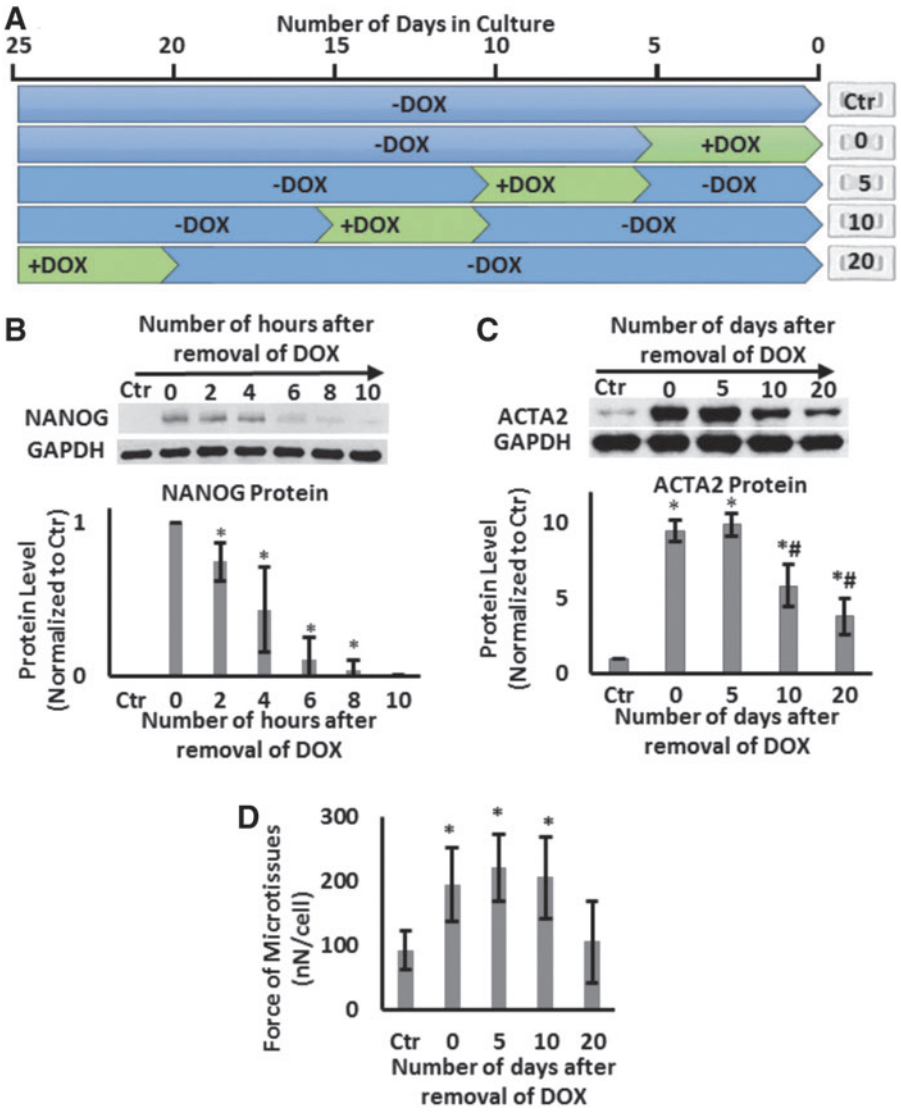

FIG. 5. The effects of NANOG persist even after DOX removal. **(A)** Schematic of the experimental design. **(B)** Western blot for NANOG and quantification of NANOG protein level as a function of time after DOX removal. **(C)** Western Blot for ACTA2 and quantification as a function of time after DOX removal. **(D)** Contractile force generated by microtissues as a function of time after DOX removal. Data are presented as mean ± standard deviation, $n = 3$ for WBs and $n = 20$ for the force measurements. * denotes $p < 0.05$ compared with control; # denotes $p < 0.05$ compared with 0 days.

manner. Recent studies in our laboratory showed that senescent cells lose their capacity to respond to TGF-β1 and that NANOG restores this deficit.[25,30] These data may explain the combined effects of NANOG and TGF-β1 on actin filament formation and restoration of the contractile capacity in aged cells.

Almost 48 h after removal of DOX from the media, the mRNA levels of ACTA2 and other myogenic markers decreased to baseline. Since NANOG was shown to have a short half-life in the cell (2.5 ± 0.5 h), this result might suggest that the presence of NANOG was necessary to maintain the transcription of myogenic markers. However, the protein level and filamentous organization of ACTA2 were sustained for several days in the absence of NANOG. Degradation of actin filaments is a multistep process, starting with disassembly of actin filaments by cytosolic proteases such as caspases and calpains,[47–49] and followed by ubiquitination and degradation of actin monomers in the proteasome.[50] It is also known that binding of actin and myosin protects them from ubiquitination and degradation. Therefore, degradation of the contractile machinery occurs at a slow pace,[51] which may explain the strong contractile function of microtissues up to 10 days after termination of NANOG expression.

In summary, our data suggest that ectopic expression of the embryonic transcription factor NANOG restored actin polymerization and the contractile function of senescent MSC-derived SMCs, suggesting that NANOG may be used to enhance the contractile properties of tissue-engineered constructs containing SMCs, such as bladder and arteries.[52–54] Given the effects of NANOG on SMC differentiation and contractile function, it is possible that NANOG might also affect the contractile function of other types of muscles such as cardiac or skeletal muscle. If true, NANOG could be used to restore the impaired contractile capacity of senescent myoblasts and repair the skeletal muscle function, which is severely compromised by aging. This hypothesis is currently under investigation in our laboratory. Finally, the senescent microtissue arrays enable high-throughput screening strategies to identify genes and pathways that are involved in reversing cellular senescence or to facilitate the development of novel antiaging treatments.

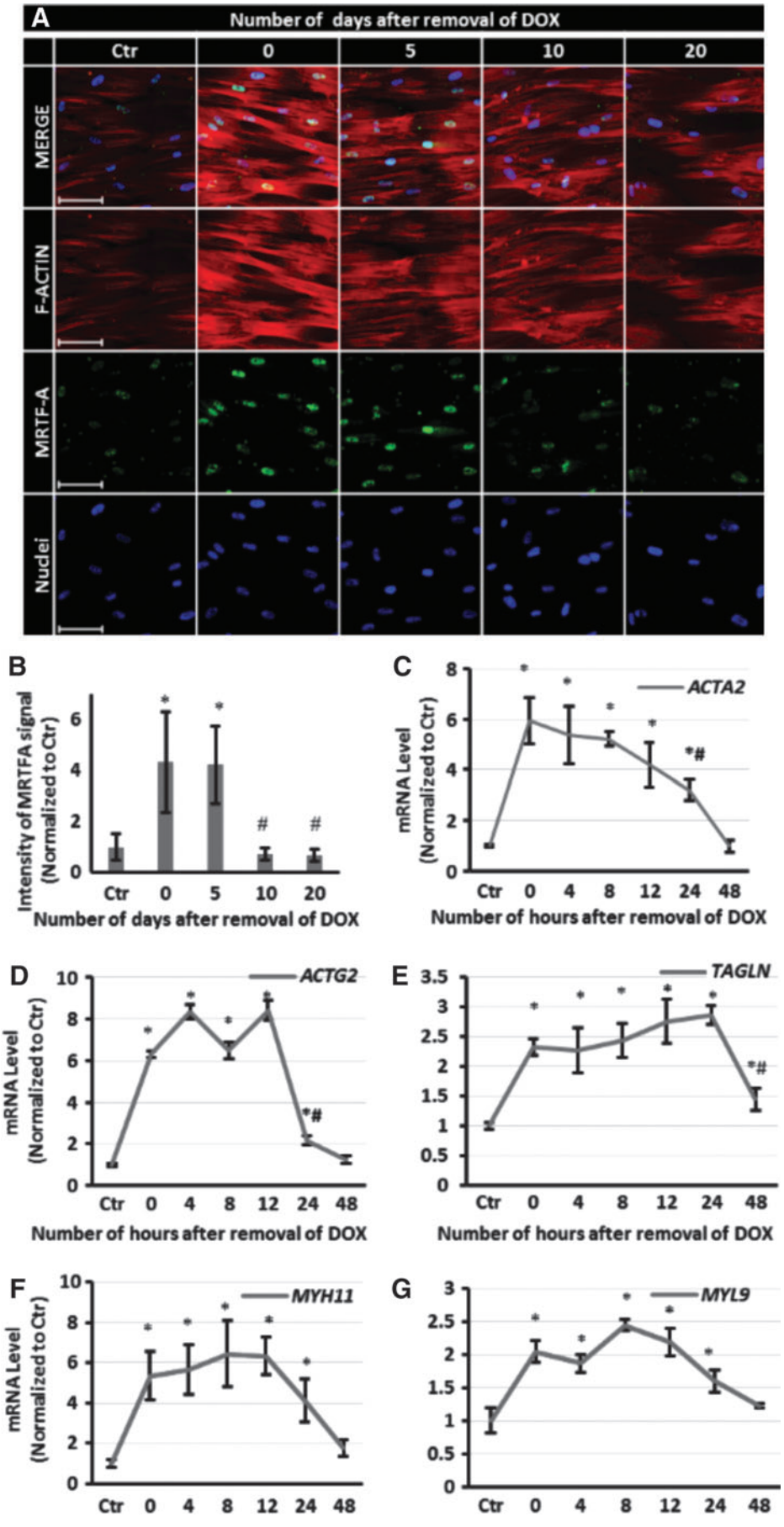

FIG. 6. MRTF-A nuclear localization, actin filament organization, and myogenic gene expression following DOX withdrawal. **(A)** Immunostaining for MRTF-A (*green*) and F-actin (*red*) as a function of time after DOX removal (scale bar = 100 μm). **(B)** Quantification of nuclear MRTFA. Intensity values are normalized to the Ctr level. **(C–G)** Quantitative RT-PCR for *ACTA2*, *ACTG2*, *TAGLN*, *MYH11*, and *MYL9* as a function of time after DOX removal. Data are presented as mean ± standard deviation, $n = 3$. * denotes $p < 0.05$ compared with control and # denotes $p < 0.05$ compared with 0 days. Ctr, control.

Acknowledgment

This work was supported by a grant from the National Institutes of Health (R01 HL086582) to S.T.A.

Disclosure Statement

STA is co-founder of Angiograft LLC, a startup company that aims at developing and commercializing cell-free vascular grafts for arterial and venous replacement therapies. No other competing financial interests exist.

References

1. Alagesan, S., and Griffin, M.D. Autologous and allogeneic mesenchymal stem cells in organ transplantation: what do we know about their safety and efficacy? Curr Opin Organ Transplant **19,** 65, 2014.
2. Griffin, M.D., Elliman, S.J., Cahill, E., English, K., Ceredig, R., and Ritter, T. Concise review: adult mesenchymal stromal cell therapy for inflammatory diseases: how well are we joining the dots? Stem Cells **31,** 2033, 2013.
3. Malgieri, A., Kantzari, E., Patrizi, M.P., and Gambardella, S. Bone marrow and umbilical cord blood human mesenchymal stem cells: state of the art. Int J Clin Exp Med **3,** 248, 2010.
4. Meirelles Lda, S., and Nardi, N.B. Methodology, biology and clinical applications of mesenchymal stem cells. Front Biosci **14,** 4281, 2009.
5. Stenderup, K., Justesen, J., Clausen, C., and Kassem, M. Aging is associated with decreased maximal life span and accelerated senescence of bone marrow stromal cells. Bone **33,** 919, 2003.
6. Baxter, M.A., Wynn, R.F., Jowitt, S.N., Wraith, J.E., Fairbairn, L.J., and Bellantuono, I. Study of telomere length reveals rapid aging of human marrow stromal cells following in vitro expansion. Stem Cells **22,** 675, 2004.
7. Hacia, J.G., Lee, C.C., Jimenez, D.F., Karaman, M.W., Ho, V.V., Siegmund, K.D., and Tarantal, A.F. Age-related gene expression profiles of rhesus monkey bone marrow-derived mesenchymal stem cells. J Cell Biochem **103,** 1198, 2008.
8. Han, J., Liu, J.Y., Swartz, D.D., and Andreadis, S.T. Molecular and functional effects of organismal ageing on smooth muscle cells derived from bone marrow mesenchymal stem cells. Cardiovasc Res **87,** 147, 2010.
9. Scruggs, B.A., Semon, J.A., Zhang, X., Zhang, S., Bowles, A.C., Pandey, A.C., Imhof, K.M., Kalueff, A.V., Gimble, J.M., and Bunnell, B.A. Age of the donor reduces the ability of human adipose-derived stem cells to alleviate symptoms in the experimental autoimmune encephalomyelitis mouse model. Stem Cells Transl Med **2,** 797, 2013.
10. Wagner, W., Horn, P., Castoldi, M., Diehlmann, A., Bork, S., Saffrich, R., Benes, V., Blake, J., Pfister, S., Eckstein, V., and Ho, A.D. Replicative senescence of mesenchymal stem cells: a continuous and organized process. PLoS One **3,** e2213, 2008.
11. Bonab, M.M., Alimoghaddam, K., Talebian, F., Ghaffari, S.H., Ghavamzadeh, A., and Nikbin, B. Aging of mesenchymal stem cell in vitro. BMC Cell Biol **7,** 14, 2006.
12. Wheeler, J.B., Mukherjee, R., Stroud, R.E., Jones, J.A., and Ikonomidis, J.S. Relation of murine thoracic aortic structural and cellular changes with aging to passive and active mechanical properties. J Am Heart Assoc **4,** e001744, 2015.
13. Ragnauth, C.D., Warren, D.T., Liu, Y., McNair, R., Tajsic, T., Figg, N., Shroff, R., Skepper, J., and Shanahan, C.M. Prelamin A acts to accelerate smooth muscle cell senescence and is a novel biomarker of human vascular aging. Circulation **121,** 2200, 2010.
14. Matthews, C., Gorenne, I., Scott, S., Figg, N., Kirkpatrick, P., Ritchie, A., Goddard, M., and Bennett, M. Vascular smooth muscle cells undergo telomere-based senescence in human atherosclerosis: effects of telomerase and oxidative stress. Circ Res **99,** 156, 2006.
15. Saphirstein, R.J., and Morgan, K.G. The contribution of vascular smooth muscle to aortic stiffness across length scales. Microcirculation **21,** 201, 2014.
16. Zieman, S.J., Melenovsky, V., and Kass, D.A. Mechanisms, pathophysiology, and therapy of arterial stiffness. Arterioscler Thromb Vasc Biol **25,** 932, 2005.
17. Wang, M., Jiang, L., Monticone, R.E., and Lakatta, E.G. Proinflammation: the key to arterial aging. Trends Endocrinol Metab **25,** 72, 2014.
18. Davis, R., Pillai, S., Lawrence, N., Sebti, S., and Chellappan, S.P. TNF-alpha-mediated proliferation of vascular smooth muscle cells involves Raf-1-mediated inactivation of Rb and transcription of E2F1-regulated genes. Cell Cycle **11,** 109, 2012.
19. Goetze, S., Xi, X.P., Kawano, Y., Kawano, H., Fleck, E., Hsueh, W.A., and Law, R.E. TNF-alpha-induced migration of vascular smooth muscle cells is MAPK dependent. Hypertension **33,** 183, 1999.
20. Manea, A., Manea, S.A., Gafencu, A.V., Raicu, M., and Simionescu, M. AP-1-dependent transcriptional regulation of NADPH oxidase in human aortic smooth muscle cells: role of p22phox subunit. Arterioscler Thromb Vasc Biol **28,** 878, 2008.
21. Bajpai, V.K., and Andreadis, S.T. Stem cell sources for vascular tissue engineering and regeneration. Tissue Eng Part B Rev **18,** 405, 2012.
22. Caplan, A.I. Adult mesenchymal stem cells for tissue engineering versus regenerative medicine. J Cell Physiol **213,** 341, 2007.
23. Peng, H.-F., Liu, J.Y., Andreadis, S.T., and Swartz, D.D. Hair follicle-derived smooth muscle cells and small intestinal submucosa for engineering mechanically robust and vasoreactive vascular media. Tissue Eng Part A **17,** 981, 2011.
24. Mistriotis, P., and Andreadis, S.T. Hair follicle: a novel source of multipotent stem cells for tissue engineering and regenerative medicine. Tissue Eng Part B Rev **19,** 265, 2013.
25. Han, J., Mistriotis, P., Lei, P., Wang, D., Liu, S., and Andreadis, S.T. Nanog reverses the effects of organismal aging on mesenchymal stem cell proliferation and myogenic differentiation potential. Stem cells (Dayton, Ohio) **30,** 2746, 2012.
26. Do, J.T., and Schöler, H.R. Regulatory circuits underlying pluripotency and reprogramming. Trends Pharmacol Sci **30,** 296, 2009.
27. Legant, W.R., Pathak, A., Yang, M.T., Deshpande, V.S., McMeeking, R.M., and Chen, C.S. Microfabricated tissue gauges to measure and manipulate forces from 3D microtissues. Proc Natl Acad Sci **106,** 10097, 2009.
28. Bajpai, V.K., Mistriotis, P., and Andreadis, S.T. Clonal multipotency and effect of long-term in vitro expansion on differentiation potential of human hair follicle derived mesenchymal stem cells. Stem Cell Res **8,** 74, 2012.
29. Bajaj, B., Lei, P., and Andreadis, S.T. High efficiencies of gene transfer with immobilized recombinant retrovirus: kinetics and optimization. Biotechnol Prog **17,** 587, 2001.
30. Mistriotis, P., Bajpai, V.K., Wang, X., Rong, N., Shahini, A., Asmani, M., Liang, M.-S., Wang, J., Lei, P., Liu, S., Zhao, R., and Andreadis, S.T. NANOG reverses the myogenic differentiation potential of senescent stem cells by restoring ACTIN filamentous organization and SRF-dependent gene expression. Stem Cells 2017;35:207–221.

31. Padmashali, R.M., Mistriotis, P., Liang, M.S., and Andreadis, S.T. Lentiviral arrays for live-cell dynamic monitoring of gene and pathway activity during stem cell differentiation. Mol Ther **22,** 1971, 2014.
32. Wang, D., Park, J.S., Chu, J.S., Krakowski, A., Luo, K., Chen, D.J., and Li, S. Proteomic profiling of bone marrow mesenchymal stem cells upon transforming growth factor beta1 stimulation. J Biol Chem **279,** 43725, 2004.
33. Kinner, B., Zaleskas, J.M., and Spector, M. Regulation of smooth muscle actin expression and contraction in adult human mesenchymal stem cells. Exp Cell Res **278,** 72, 2002.
34. Liu, J.Y., Peng, H.F., Gopinath, S., Tian, J., and Andreadis, S.T. Derivation of functional smooth muscle cells from multipotent human hair follicle mesenchymal stem cells. Tissue Eng Part A **16,** 2553, 2010.
35. Olson, E.N., and Nordheim, A. Linking actin dynamics and gene transcription to drive cellular motile functions. Nat Rev Mol Cell Biol **11,** 353, 2010.
36. Dehghanifard, A., Shahjahani, M., Soleimani, M., and Saki, N. The emerging role of mesenchymal stem cells in tissue engineering. Int J Hematol Oncol Stem Cell Res **7,** 46, 2013.
37. Westerweel, P.E., and Verhaar, M.C. Directing myogenic mesenchymal stem cell differentiation. Circ Res **103,** 560, 2008.
38. Liu, J.Y., Peng, H.F., and Andreadis, S.T. Contractile smooth muscle cells derived from hair-follicle stem cells. Cardiovasc Res **79,** 24, 2008.
39. Wang, C., Yin, S., Cen, L., Liu, Q., Liu, W., Cao, Y., and Cui, L. Differentiation of adipose-derived stem cells into contractile smooth muscle cells induced by transforming growth factor-beta1 and bone morphogenetic protein-4. Tissue Eng Part A **16,** 1201, 2010.
40. Liang, M.S., and Andreadis, S.T. Engineering fibrin-binding TGF-beta1 for sustained signaling and contractile function of MSC based vascular constructs. Biomaterials **32,** 8684, 2011.
41. Alimperti, S., You, H., George, T., Agarwal, S.K., and Andreadis, S.T. Cadherin-11 regulates both mesenchymal stem cell differentiation into smooth muscle cells and the development of contractile function in vivo. J Cell Sci **127,** 2627, 2014.
42. Engler, A.J., Sen, S., Sweeney, H.L., and Discher, D.E. Matrix elasticity directs stem cell lineage specification. Cell **126,** 677, 2006.
43. Riehl, B.D., Park, J.-H., Kwon, I.K., and Lim, J.Y. Mechanical stretching for tissue engineering: two-dimensional and three-dimensional constructs. Tissue Eng Part B Rev **18,** 288, 2012.
44. Koobatian, M.T., Liang, M.S., Swartz, D.D., and Andreadis, S.T. Differential effects of culture senescence and mechanical stimulation on the proliferation and leiomyogenic differentiation of MSC from different sources: implications for engineering vascular grafts. Tissue Eng Part A **21,** 1364, 2015.
45. Lodish, H, Berk, A., Zipursky, S.L., *et al.* Molecular Cell Biology. New York: W.H. Freeman; 2000.
46. Aguilar, H.N., and Mitchell, B.F. Physiological pathways and molecular mechanisms regulating uterine contractility. Hum Reprod Update **16,** 725, 2010.
47. Du, J., Wang, X., Miereles, C., Bailey, J.L., Debigare, R., Zheng, B., Price, S.R., and Mitch, W.E. Activation of caspase-3 is an initial step triggering accelerated muscle proteolysis in catabolic conditions. J Clin Invest **113,** 115, 2004.
48. Kong, J.Y., and Rabkin, S.W. Cytoskeletal actin degradation induced by lovastatin in cardiomyocytes is mediated through caspase-2. Cell Biol Int **28,** 781, 2004.
49. Huang, J., and Forsberg, N.E. Role of calpain in skeletal-muscle protein degradation. Proc Natl Acad Sci U S A **95,** 12100, 1998.
50. Polge, C., Heng, A.E., Jarzaguet, M., Ventadour, S., Claustre, A., Combaret, L., Bechet, D., Matondo, M., Uttenweiler-Joseph, S., Monsarrat, B., Attaix, D., and Taillandier, D. Muscle actin is polyubiquitinylated in vitro and in vivo and targeted for breakdown by the E3 ligase MuRF1. Faseb J **25,** 3790, 2011.
51. Solomon, V., and Goldberg, A.L. Importance of the ATP-ubiquitin-proteasome pathway in the degradation of soluble and myofibrillar proteins in rabbit muscle extracts. J Biol Chem **271,** 26690, 1996.
52. Mahfouz, W., Elsalmy, S., Corcos, J., and Fayed, A.S. Fundamentals of bladder tissue engineering. Afr J Urol **19,** 51, 2013.
53. Liang, M.-S., Koobatian, M., Lei, P., Swartz, D.D., and Andreadis, S.T. Differential and synergistic effects of mechanical stimulation and growth factor presentation on vascular wall function. Biomaterials **34,** 7281, 2013.
54. Yao, L., Swartz, D.D., Gugino, S.F., Russell, J.A., and Andreadis, S.T. Fibrin-based tissue-engineered blood vessels: differential effects of biomaterial and culture parameters on mechanical strength and vascular reactivity. Tissue Eng **11,** 991, 2005.

Address correspondence to:
Stelios T. Andreadis, PhD
Bioengineering Laboratory
Department of Chemical and Biological Engineering,
University at Buffalo
The State University of New York
908 Furnas Hall
Amherst, NY 14260-4200

E-mail: sandread@buffalo.edu

Received: November 12, 2016
Accepted: January 25, 2017
Online Publication Date: February 28, 2017